# Improved Navigation and Guidance System of AUV Using Sensors Fusion

Hatem A. Khater[1], Ashraf. Elsayed[2,3], and Noha. El-Shoafy[3]
[1] Department of Mechatronics, Faculty of Engineering, Horus University, Egypt.
[2] Department of Applied Mathematics and Information Science, Zewail city of Science and Technology, Giza, Egypt
[3]Department of Mathematics and Computer Science at Faculty of Science, Alexandria University, Alexandria, Egypt
Email: {hatem.a.khater, elshoafyn}@gmail.com; ashraf.elsayed@alexu.edu.eg

***Abstract***—Improved navigation and guidance system of Autonomous Underwater Vehicle (AUV) is a most important assignment for most researchers, specifically in difficult environments such as the ocean. In ocean environment, the AUV needs a reliable navigation and guidance system to navigate and guidance AUV in the desired path with high efficiency. The proposed method for improving navigation system of AUV is based on integrated MEMS smartphone sensors by the collected data from Doppler Velocity Log (DVL), depth, and compass sensors via Loosely Coupled Kalman Filter (KF). The Loosely Coupled KF is used to estimate and correct velocity and attitude errors of AUV navigation system by DVL, depth and compass measurements, respectively. The practice device of AUV is based on Ultrasonic sensors, microcontroller, depth, and digital circuit sensors. The ultrasonic sensor is used to detect boundaries in the route of AUV. The depth sensor is used to dive the AUV in the required depth. The microcontroller and digital circuit are usage to rule the motion and direction of AUV in the required path. The AUV is examined in a testbed at depth of 7 meters from water surface. There are three obstacles are placed in the direction of AUV to check its efficiency. During tests, the AUV is capable to reach the target place with high efficiency. After that, it returned back to the base station accordance to saved direction in its reminiscence with full effectiveness also.

***Index Terms***—AUV, Smartphone MEMS Sensors, DVL, Ultrasonic sensor, Depth Sensor, Digital compass, Microcontroller and Testbed.

## I. Introduction

A reliable navigation and guidance system in ocean environment is very essential issue of most Autonomous Underwater Vehicles (AUVs) that required a particular path for Planning, guidance and autonomous navigation. In this paper, the AUV navigation system is primarily based on Micro-Electro-Mechanical System (MEMS) - Inertial Navigation (INS) of smartphone sensors [1]. Today, most updated smartphone units maintain various MEMS sensors such as accelerometers, gyroscopes, magnetometer, orientation, barometer, and so on that can be used in several applications. The MEMS accelerometers and gyroscopes sensors of the smartphone are shown in Fig. 1.

Manuscript received December 31, 2019; revised April 20, 2020.
Corresponding author email: elshoafyn@gmail.com
doi:10.12720/jcm.15.6.455-468

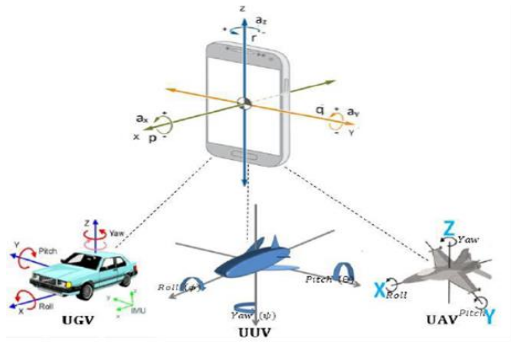


Fig. 1. Smartphone MEMS-INS sensors.

The MEMS smartphone sensors have many advantages. They can reduce cost, size and provide acceptable efficiency. The disadvantages of smartphones MEMS sensors are their errors increase over time due to accelerometers and gyroscopes drifts. This paper aims to improve the navigation system of AUV via integrated MEMS-INS smartphone sensors (3 accelerometers and 3 gyroscopes) by Doppler Velocity Log. (DVL), deepness and circuit sensors. The DVL is used to limit velocity errors, whilst deepness and circuit sensors are necessity to decrease posture errors of AUV navigation system [2]. The data collected from MEMS-INS smartphone (3 accelerometers and 3 gyroscopes), DVL, depth and compass sensors are integrated via Loosely Coupled Kalman Filter (FK). Loosely Coupled KF is used to estimate and correct velocity and attitude errors of AUV navigation system by DVL, depth and compass measurements, respectively. The guidance system of AUV is based on ultrasonic sensor, microcontroller, depth sensor, and digital compass. The ultrasonic sensor is used to realize boundaries in the path of AUV. The depth sensor is used to dive the AUV in required depth. The Arduino microcontroller is used as guidance and control system. It is used to manage the movement and path of AUV to keep away from obstacles. The digital circuit is used to adjust the movement attitude of AUV in order it pass it in the required path [3], [4].

## II. Overview of AUV Construction

The block design of AUV system with its major subsystems is shown in Fig. 2. It consists of three main subsystems as follows:

- AUV Guidance System: The guidance system is used to instruct ASV to reach the goal position to enforce the required tasks. It also saves the path taken by the AUV in its memory. The return back of AUV to base station depends on the stored direction in its memory.
- AUV Guidance System: The guidance system is used to guide ASV to reach the target position to implement the required tasks. It also saves the path taken by the AUV in its memory. The return back of AUV to base station depends on the stored path in its memory.
- AUV Control System: The control system is used to control the movement and direction of AUV to avoid obstacles.

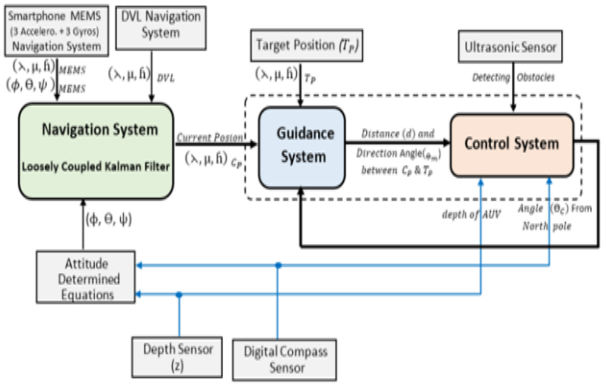


Fig. 2.Block diagram of AUV system.

### A. AUV Navigation System

The navigation system of AUV is shown in Fig. 3. The MEMS smartphone sensors (3 accelerometers and 3 gyroscopes) are used to determine the velocity and attitude of AUV. It is integrated and fused with DVL, depth and compass sensors via Loosely Coupled Kalman Filter. The DVL system is used to correct velocity errors. While deepness and compass are usage to accutate attitude errors of AUV navigation system.

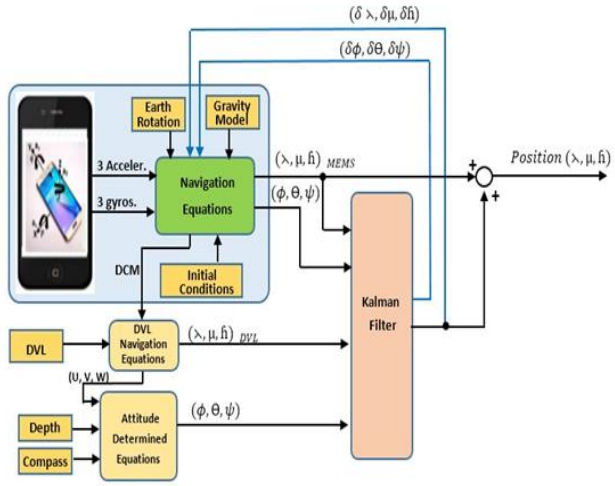


Fig. 3. AUV navigation system.

#### 1) MEM-INS navigation system

Normally, most MEMS-INS systems consist of three accelerometers and three gyroscopes to measure the accelerations ($a_x$, $a_y$, $a_y$) and angular rates (p, q, r) around three axes (x, y, z), respectively. Today, most smartphones contain several MEMS sensors such as accelerometers, gyroscopes, Camera, temperature, magnetometer, orientation, barometer and so on which can be used in several applications such as autonomous navigation and guidance. [5].

#### 2) Accelerometer

Accelerometers are common MEMS devices. They measure the rate of accelerations ($a_x$, $a_y$, and $a_z$) on three axes (x, y, z), respectively. Most an accelerometer sensors consist of a seismic mass and support spring that made of silicon as shown in Fig. 4.

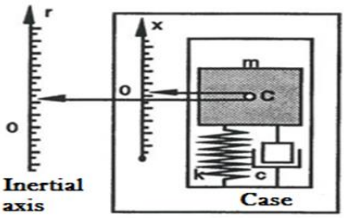


Fig. 4. Accelerometer Sensor.

The provided acceleration from an accelerometer is determined by Newton's Second Law as following Eq. (1).

$$f = ma \tag{1}$$

where f is the force, m is the mass, and a is the acceleration. Let $\vec{\boldsymbol{a}}(\boldsymbol{t})$ $\vec{\boldsymbol{v}}(\boldsymbol{t})$ and $\vec{\boldsymbol{x}}(\boldsymbol{t})$ be the acceleration, velocity, and position vectors of the vehicle, respectively. The relationships between velocity, position, and acceleration $\vec{a}(\boldsymbol{t})$ are given by following Eq. (2).

$$\vec{v}(t) = \int_0^t \vec{a}(t)dt$$

$$\vec{x}(t) = \int_0^t \vec{v}(t)dt \tag{2}$$

$$\vec{x}(t) = \int_0^t \int_0^t \vec{a}(t)dt\, d(t)$$

#### 3) Gyroscopes

The principle basics of Gyroscopes are somewhat similar to that of acceleration sensors. It is designed to measure the angular rates (r, q, and p) on three axes (x, y, and z). The gyroscopes are made of massive rotors called spin axes. They are fixed on rings called gimbals on three axes. These gimbals are designed to isolate the central rotor from any outside torques. When there are any rotations along the axis, this rotation will be detected and processed to measure the angular rate value on this axis. The principle basic of the gyroscope is shown in Fig. 5.

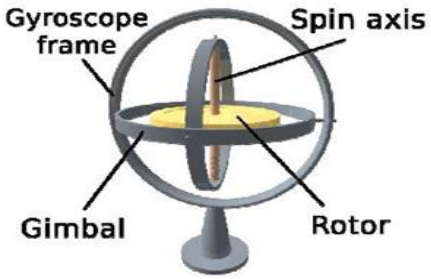


Fig. 5. Gyroscope Sensor.

### B. MEM Smartphone Navigation Equations

MEMS smartphone sensors consist of three gyroscopes and three accelerometers to determine the angular rates (p, q, r) and accelerations ($a_x$, $a_y$, $a_z$), respectively [6]. The (p, q, r) and ($a_x$, $a_y$, $a_z$) are used to determine the attitude (ϕ, θ, ψ) and velocities (U, V, W) in Vehicle Coordinate System (VCS), respectively. The attitude is used to determine the Direction Cosine Matrix (DCM). DCM is usage to transform the velocities from VCS to Navigation Coordinates System (NCS) [7]. The relation between the derivative of the Euler angles and angular rates [8] is given by using Eq. (3).

$$\begin{bmatrix}\dot{\phi}\\ \dot{\theta}\\ \dot{\psi}\end{bmatrix}=\begin{bmatrix}1 & \sin\phi\tan\theta & \cos\phi\tan\theta\\ 0 & \cos\phi & -\sin\phi\\ 0 & \sin\phi/\cos\theta & \cos\phi/\cos\theta\end{bmatrix}\begin{bmatrix}p\\ q\\ r\end{bmatrix} \quad (3)$$

By integration, the Eq. (3) gives attitude ($\phi, \theta, \psi$) using the initial conditions of attitude at a given time.

The accelerations of the vehicle along the three body axes are determined by MEMS smartphone accelerometers. If the acceleration due to gravity ($g$) is supplied as a function of location around the earth [9], then $U$, $V$, and $W$ are given by Eq. (4).

$$\begin{aligned}\dot{U} &= a_x + rV - qW + g\sin\theta\\ \dot{V} &= a_y - rU + pW - g\cos\theta\sin\phi\\ \dot{W} &= a_z + qU - pV - g\cos\theta\cos\phi\end{aligned} \quad (4)$$

By integration, the Eq. (4) gives velocities (U, V and W) in VCS body using the initial velocities. The DCM is usage to transform the velocities (U, V, W) from VCS body to velocities ($V_N$, $V_E$, $V_D$) in North -East-Down (NED) body. It is given by using Eq. (5).

DCM=

$$\begin{bmatrix}\cos\theta\cos\psi & \cos\theta\sin\psi & -\sin\theta\\ \sin\theta\sin\phi\cos\psi-\sin\psi\cos\phi & \sin\phi\sin\theta\sin\phi+\cos\psi\cos\phi & \sin\phi\cos\theta\\ \sin\theta\cos\phi\cos\psi+\sin\psi\sin\phi & \sin\phi\sin\theta\cos\phi-\cos\psi\sin\theta & \cos\phi\cos\theta\end{bmatrix} \quad (5)$$

The relationship among the velocities (U, V, W) in VCS frame and velocities ($V_N$, $V_E$, $V_D$) in NED frame is given by Eq.(6).

$$\begin{bmatrix}V_N\\ V_E\\ V_U\end{bmatrix}_{INS}=DCM^T\begin{bmatrix}U\\ V\\ W\end{bmatrix}_{INS} \quad (6)$$

The geodetic (latitude, longitude, altitude) frame is used as navigation frame. Let ⋋, μ and ℏ denote the latitude, longitude and altitude of the vehicle at any instant, respectively. The relationship between velocities ($V_N$, $V_E$, $V_D$) in NED frame and geodetic frame can be expressed by Eq. (7).

$$\begin{bmatrix}\dot{\lambda}\\ \dot{\mu}\\ \dot{\hbar}\end{bmatrix}_{INS}=\begin{bmatrix}\frac{1}{Re} & 0 & 0\\ 0 & \frac{1}{Re\cos\lambda} & 0\\ 0 & 0 & -1\end{bmatrix}\begin{bmatrix}V_N\\ V_E\\ V_U\end{bmatrix}_{MEMS} \quad (7)$$

where Re is the radius of the earth. By integration, the Eq. (7) gives the position (⋋, μ, ℏ) in geodetic body the use of the initial situation of a position at a given time. The block diagram of MEMS smartphone navigation equations is shown in Fig. 6.

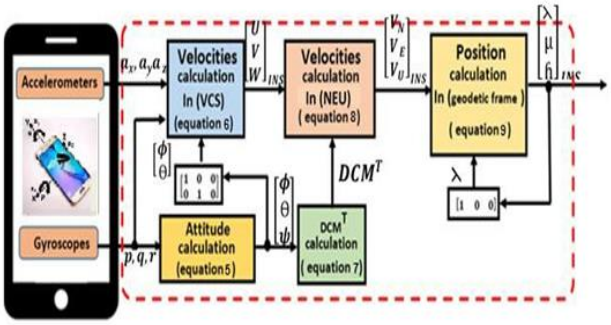


Fig. 6. Block diagram of MEMS navigation equations.

The Fig. 7 shows the relationship between common references frames that used in navigation frames. They include Earth Central Earth Fixed (ECEF) frame, North - East-Up (NEU) frame and geodetic (⋋, μ, ℏ) frame.

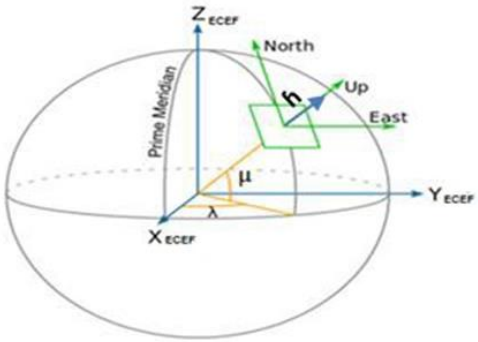


Fig. 7. Relationship between references frames commonly used in inertial navigation.

### C. DVL Navigation System

MEMS smartphone sensors (3 accelerometers and 3 gyroscopes) have a good short-term accuracy and they provide a continuous navigation solution, but their errors are increasing over time. To avoid this disadvantage, the MEMS smartphone sensors are fused and integrated by DVL to reduce velocity errors of AUV. Most DVL has 4 transducers as shown in Fig. 8. Only one transducer is used as an emitter and three remained transducers are usage to measurement velocities (U, V, and W) on three axes (x, y, and z), respectively [10].

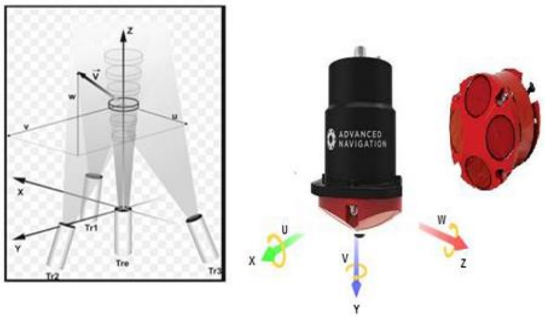


Fig. 8. DVL fundamentals.

The measured velocity by DVL is given by Eq.(8)

$$V_{DVL} = \frac{\Delta f \; C_{sound}}{2 \; f_0 \; cos(\theta_{dvl})} \quad (8)$$

where: $V_{dvl}$ is the velocity of the vehicle along the axis, $\Delta f$ is the difference between transmitter frequencies and reflect frequency, $f_0$ is transmitted frequency, $f_r$ is reflected frequency, $c_{sound}$ is the speed of the sound in water, and $\Theta_{dvl}$ is the angle transmission between $L_1$ and $L_2$ level. The angle transmission angle between $L_1$ and $L_2$ is given by Eq. (9) and shown in Fig. 9.

$$\tan(\theta_{dvl}) = \frac{L_2}{L_1} \quad (9)$$

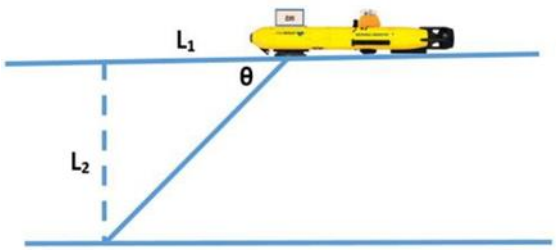


Fig. 9. Transmission angle between L1 and L2.

*1) DVL navigation equations*

The DVL measurements are used to reduce velocities errors of AUV navigation system. Therefore, the integration between MEMS smartphone and DVL is a Key step in reducing errors of navigation system [11], [12]. Before integrated MEMS smartphone sensors with DVL, the MEMS smartphone sensors and DVL must be located at the same level on the body of ASV as shown in figure 10. In this case, the same DCM can be used to convert the determined velocities by MEMS smartphone and DVL from VCS to NCS frame.

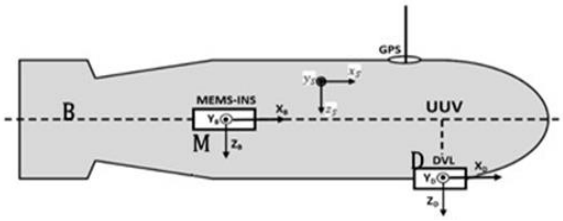


Fig. 10. MEMS and DVL levels relative to the ASV body.

The converted velocities of DVL form VCS frame to velocities ($V_N$, $V_E$, $V_U$) in NED frame are given by Eq. (10).

$$\begin{bmatrix} V_N \\ V_E \\ V_U \end{bmatrix}_{DVL} = DCM^T \begin{bmatrix} U \\ V \\ W \end{bmatrix}_{DVL} \quad (10)$$

The relationship between velocities ($V_N$, $V_E$, $V_D$) in NED frame and velocities ($\dot{\lambda}$, $\dot{\mu}$, $\dot{h}$) in the geodetic frame is given by Eq. (11).

$$\begin{bmatrix} \dot{\lambda} \\ \dot{\mu} \\ \dot{h} \end{bmatrix}_{DVL} = \begin{bmatrix} \frac{1}{Re} & 0 & 0 \\ 0 & \frac{1}{Re \cos\lambda} & 0 \\ 0 & 0 & -1 \end{bmatrix} \begin{bmatrix} V_N \\ V_E \\ V_U \end{bmatrix}_{DVL} \quad (11)$$

By integration, the Eq. (11) shows the geodetic frame location using initial position state at a given time.

*D. Determined Attitude Equations*

A determined attitude ($\phi$, $\Theta$, $\psi$) by MEMS smartphone (Eq. (3)) is used to create DCM matrix that using to convert velocities of MEMS and DVL from VCS to NCS. But this attitude has errors increase with time due to the gyroscope drifts [13]. [14].So the attitude errors in our proposed method are corrected by depth (z) and compass ($\psi$) measurements. The Depth sensor measures the depth (z) of the vehicle from the surface using pressure transducer [15], [16]. The depth (z) value can measure by the Eq. (12).

$$Z = \frac{Pa - P_0}{Pg} \quad (12)$$

where z is the depth value with meter (m), $P_0$ is the pressure at current depth point, $P_a$ is the atmospheric pressure at the surface, $\rho$=1030kg/m$^3$ is the water density, and $g$=9.8 m/s is the gravity. The derivative of quaternions ($\dot{q_0}$, $\dot{q_1}$, $\dot{q_2}$, $\dot{q_3}$) and angular rates (p, q, r) is given by Eq. (13).

$$\begin{pmatrix} \dot{q}_0 \\ \dot{q}_1 \\ \dot{q}_2 \\ \dot{q}_3 \end{pmatrix} = \begin{pmatrix} 0 & -p/2 & -q/2 & -r/2 \\ p/2 & 0 & r/2 & -q/2 \\ q/2 & -r/2 & 0 & q/2 \\ r/2 & q/2 & -p/2 & 0 \end{pmatrix} \begin{pmatrix} q_0 \\ q_1 \\ q_2 \\ q_3 \end{pmatrix} \quad (13)$$

The relationship between the changed in z and (q) quaternions is given by Eq. (14).

$$Z = 2(q_1 q_3 - q_0 q_2)U + 2(q_0 q_1 - q_2 q_3)V + (q_0^2 - q_1^2 - q_{2+}^2 q_3^2)W \quad (14)$$

where U, V and W are the speeds calculated from the DVL. The attitude estimated by quaternions method, is given by Eq. (15).

$$\begin{aligned} \emptyset &= a\tan 2(2(q_0 q_1 + q_2 q_3), 1 - 2(q_1^2 + q_2^2)) \\ \theta &= \arcsin 2 (q_0 q_2 - q_3 q_1) \\ \emptyset &= a\tan 2(2(q_0 q_3 + q_1 q_{23}), 1 - 2(q_2^2 + q_3^2)) \end{aligned} \quad (15)$$

The partial derivatives of $\dot{z}$ with respect to the quaternions, is given by Eq. (16).

$$\begin{aligned} \frac{\partial \acute{z}}{\partial q_0} &= -2 q_2 V + 2 q_1 V + 2 q_0 W \\ \frac{\partial \acute{z}}{\partial q_1} &= -2 q_3 U + 2 q_0 V + 2 q_1 W \\ \frac{\partial \acute{z}}{\partial q_2} &= -2 q_0 U + 2 q_3 V + 2 q_2 W \\ \frac{\partial \acute{z}}{\partial q_3} &= -2 q_1 U + 2 q_2 V + 2 q_3 W \end{aligned} \quad (16)$$

The simplified of Eq. (14) is given by Eq. (17).

$$\acute{Z} = -\sin\theta.U + \sin\emptyset\cos\dot{\theta}.V + \cos\emptyset\cos\theta.W \quad (17)$$

From Eq. (17), only the angle of roll ($\phi$) and pitch ($\Theta$) can be corrected by deepness (z). So to fix the yaw angle ($\psi$) the compass is used. The compass is among the oldest navigation devices that ship commanders, pilots and explorers are still using widely [17]. A compass consists of two sensors to calculate the Earth's magnetic field change on two axes (X, Y) relative to the North Pole as shown in figure 11.

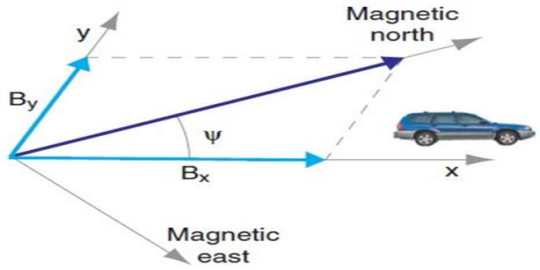


Fig. 11. Principle basic of compass sensor.

If $B_X$ and $B_Y$ are adjustments made in the magnetic domain on the X and Y axes, respectively, then the compass angle will give by Eq. (18).

$$\varphi_{compass} = arctan\left(\frac{B_Y}{B_X}\right) \quad (18)$$

### E. Kalman Filter

The Kalman filter (KF) is a calculation algorithm that recursively works based on the basis of initial estimates and prior knowledge. The Kalman filter assumes that the dynamics of the navigation system are discrete in time. It comes as a result of two stages, the stage of prediction stage and the stage of updating [18].

Based on values obtained from the prior period (k-1), the state vector ($\hat{x}_k$) and the error co-variance matrix ($P_k$) of the present period (k) are estimated prediction phase. This relation is given by Eq. (19).

$$\hat{x}_k^- = f(k, \hat{x}_{k-1}^+) \quad (19)$$

where $f(k,x)$ is the integral of dynamics matrix .The error covariance matrix ($P_k$) is given by Eq. (20):

$$P_k^- = F_{k-1}P_{k-1}F_{k-1}^T + Q_k \quad (20)$$

where $F_k$ denotes the system dynamics matrix and $Q_k$ is a spectral density matrix.

**In the update stage**, Kalman gains ($K_K$) that is given by Eq. (21):

$$K_k = P_k^- H_k^T (H_k P_k^- H_k^T + R_k)^{-1} \quad (21)$$

where $H_K$ is an observation matrix and $R_k$ is matrix for noise calculation. The state vector ($\hat{x}_k$) will be modified with the following Eq. (22):

$$\hat{x}_k^+ = \hat{x}_k^- + K_k z_k - h(k, \hat{x}_x^-) \quad (22)$$

where $z_k$ is the vector of measure and $h(k,x)$ is an integral matrix of observation ($H_K$). The error covariance matrix is then updated using the following Eq. (23):

$$P_k^+ = P_k^- - K_k H_k P_k^- \quad (23)$$

Previous knowledge such as matrix of transition ($\phi_k$), noise covariance matrix ($Q_k$), observation matrix ($H_k$), shaping matrix ($G_k$), and measuring noise matrix ($R_k$) must be calculated prior to the beginning of the test. Taylor's series expansion may be used to expand the transition matrix($\Phi_k$). It is given by Eq. (24):

$$\Phi_k = exp(F_{k-1}\mathcal{T}_i) \approx I + F\mathcal{T}_i \quad (24)$$

where I is identity matrix and $\mathcal{T}_i$ is time variable. The noise matrix ($Q_K$) is given by Eq. (25):

$$Q_k = diag\left(n_{rg}^2 I_3 n_{ra}^2 I_3 0_3 n_{bad}^2 I_3 n_{bdg}^2 I_3\right)\tau_i \quad (25)$$

where $I_3$ is an identity matrix (3 x 3), $n_{rg}^2$ is the angular rate error Power Spectrum Density (PSD), $n_{ra}^2$ is the PSD of speed error, $n_{bad}^2$ is the accelerometer bias instability PSD, and $n_{bgd}^2$ is the gyroscope bias instability PSD.The observation matrix ($H_k$) is given by Eq. (26):

$$H_k = \begin{pmatrix} 0_3 & 0_3 & -I_3 & 0_3 & 0_3 \\ 0_3 & -I_3 & 0_3 & 0_3 & 0_3 \end{pmatrix}_k \quad (26)$$

where $0_3$ is a (3 x 3) Zero matrix. The shaping matrix ($G_k$) is given by Eq. (27):

$$G_k = \begin{pmatrix} C_b^n & 0_3 \\ 0_3 & C_b^n \\ 0_{9x3} & 0_{9x3} \end{pmatrix} \quad (27)$$

where $C_b^n$ is rotating matrix, that converts errors of the INS frame $(b)$ to navigation frame $(n)$.

The central measurement noise square ($v_k$) is the noise control matrix ($R_k$). It is given by Eq. (28):

$$R_k = E\,(v_k v_k^T) \quad (28)$$

The error of the state variable and measurement function is determined in the concept of state-space. The dynamic system ($\dot{x}_k$) of the KF model is given by Eq. (29):

$$\dot{x}_k = f(\hat{x}_k) + G_k w_k \quad (29)$$

where $w_k$ is process noise of MEMS smartphone sensors. The measurement vector($z_k$) of the KF model is given by Eq. (30):

$$z_k = \begin{pmatrix} P_{ins}^n - & P_{dvl}^n \\ V_{ins}^n - & V_{dvl}^n \end{pmatrix} \quad (30)$$

where $p^n$ and $v^n$ are position and velocity of respectively in the navigation frame.

### F. MEMS /DVL/Depth/Compass Integrated System of AUV

The navigation model of AUV is designed with Matlab and Simulink as shown in Fig. 12. It consists of two stages.

The first stage consists of collection and fusion data measurements from smartphone MEMS, DVL, Depth and compass sensors. The second stage consists of integrated MEMS smartphone with DVL, depth and compass via Loosely Coupled Kalman [19], [20].

The state vectors ($\phi$, $\Theta$, $\psi$ ) MEMS that determined by MEMS smartphone navigation equation (Eq. (3)) are

integrated by state vectors (ϕ, Θ, ψ ) MEMS that determined by depth and compass equations (Eq. (17) & Eq. (18)) via Loosely Coupled KF to estimate and correct attitude errors.

In the same time, the state vectors (ʎ, μ, ɦ) MEMS that determined by MEMS smartphone navigation equation (Eq. (7)) are integrated by state vectors (ʎ, μ, ɦ) DVL that determined by DVL navigation equation (Eq. (11)) via Loosely Coupled KF to estimate and correct velocity errors.

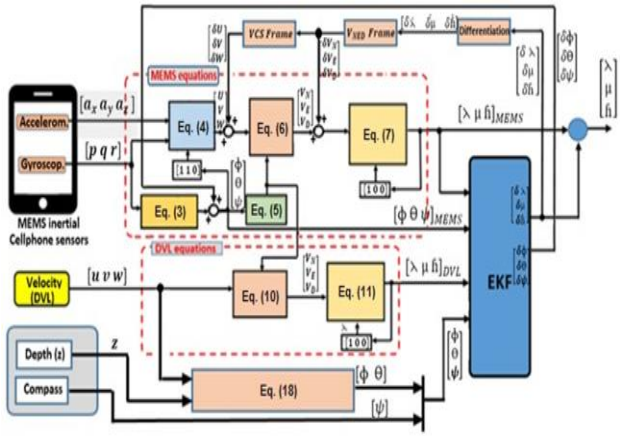


Fig. 12. Software model of MEMS/DVL/Depth/Compass Loosely Coupled KF.

## III. Guidance & Control System of AUV

The core aspects of the command and direction system are a microcontroller, ultrasonic, depth, and, digital compass sensors. They are used to control the movement and direction of AUV to avoid obstacles and guide AUV in the desired path.

### A. Control System of AUV

The control system of AUV consists of the following parts:

*1) Arduino microcontroller*

The Arduino Uno is a microcontroller system built on the ATmega328 chip as shown in Fig. 13.

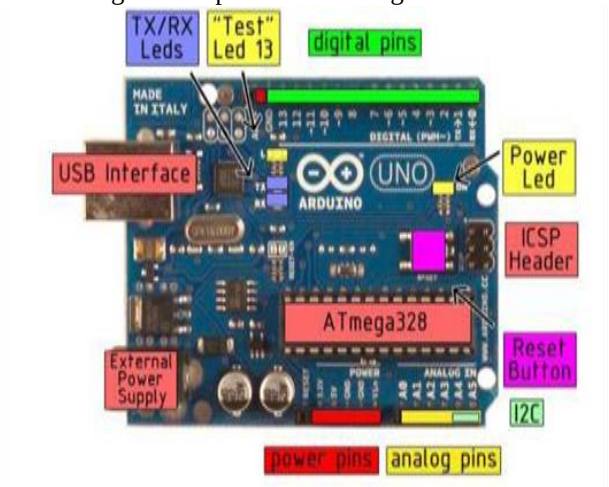


Fig. 13. Arduino microcontroller.

It is a programmable open source tool designing interactive works [21]. It has several advantages as follows:-

- It can power AUV engines, LEDs, sensors and other items.
- It is a computer system of smaller size that requires low power with high precision, and to most Unmanned Vehicles (UVs) it is a suitable processing platform.
- It comprises of a microchip of read-write capacities on a computer chip, memory, inputs, and outputs.

Arduino microcontroller is used as a control and guidance system. It is used to process the measured data of sensors to control the movement and direction of ASV. The data sheet of the Arduino microcontroller is given in Table I.

Table I: Arduino Microcontroller Data Sheet

| Microcontroller | ATmega328 |
|---|---|
| Operating Voltage | 5V |
| Input Voltage (recommended) | 7-9V |
| Output Voltage (recommended) | 6-20V |
| Digital I/O Pins | 14(of which 6 provide PWM output) |
| Analog Input Pins | 6 |
| DC Current per I/O Pin | 40 mA |
| DC Current for 3.3V Pin | 50 mA |
| Flash Memory | 32 KB (ATmega328)<br>(0.5 KB used by boot loader) |
| SRAM | 2 KB (ATmegs328) |
| EEPROM | 1 KB (ATmegs328) |
| Clock Speed | 16 MHZ |

*2) Accelerate and command direction of AUV*

The process for controlling AUV rate is the Pulse Width Modulation (PWM) method [22]. The PWM produces a rectangular pulse wave which results in variation of the y (t) average waveform value as shown in Fig. 14. The average value of y (t) waveform is given by Eq. (31).

$$\bar{y} = \frac{1}{T}\int_0^T y(t)\,dt \tag{31}$$

where: $\bar{y}$ is the average value of y (t) waveform, T is periodic time.

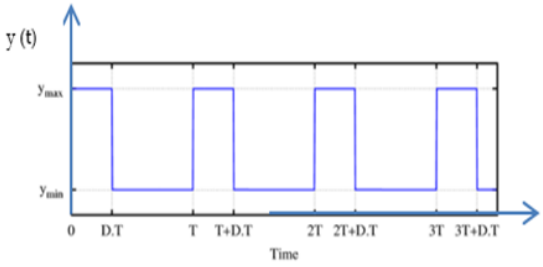


Fig. 14. Pulse waveform.

y (t) is a rectangular pulse wave. It is given by Eq. (32).

$$y(t) = \begin{pmatrix} y_{max}, for & 0 < t < D * T \\ y_{min}, for & D * T < t < T \end{pmatrix} \quad (32)$$

where: $y_{max}$ is the maximum value of the waveform, $y_{min}$ is the wave form lowest possible value D is the work period. The mean value of the pulse waveform is presented by Eq. (33).

$$\bar{y} = \frac{1}{T}(D * T * y_{max} + T * y_{min}(1 - D)) \quad (33)$$

If $y_{max}$ = 0 and $y_{min}$ = 1, then Eq. (34) gives the average value.

$$\bar{y} = D \quad (34)$$

Fig. 15 shows examples of the median value for varying D.

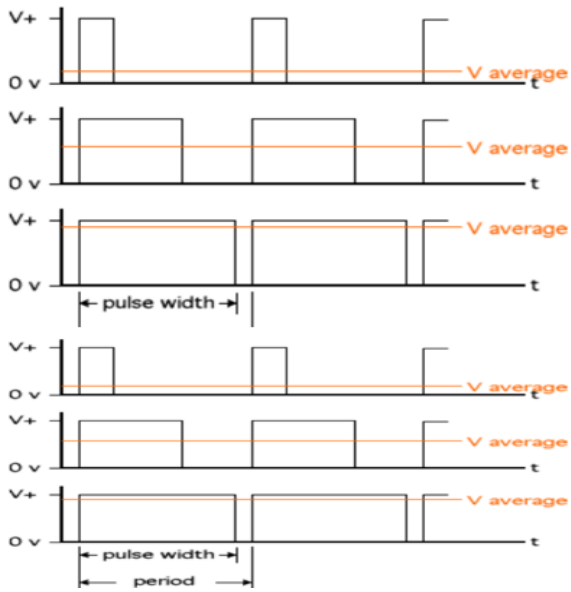


Fig. 15. Waveform for different values of D.

*3) The sensors ultrasonic*

An ultrasonic sensor concept is comparable to the radar and sonar concept. It usually consists of the sensor transmitter and the sensor receiver [23]. The sender sensor sends sound waves of high frequency and by its receiver sensor measures the reflected echo from the obstruction. As shown in figure 16, the time interval between sending and receiving signal will be used to evaluate the distance between the obstacle and the AUV.

In several other implementations, this technique could be used to measure a speed, distance, detect and avoid obstacles.

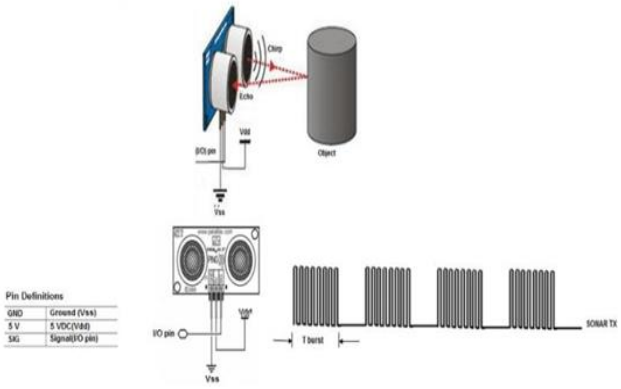


Fig. 16. Principle of parallax PING ultrasonic sensor.

Many Ultrasonic sensors have a burst pulse frequency ($f_{burst}$) of around 40 kHz. And Eq. (35) gives the length of the sound wave.

$$\lambda = C_s / f_{burst} \quad (35)$$

In which $C_s$ is sound velocity and $f_{burst}$ would be the ultrasonic burst pulse frequency. Eq. (36) gives the wavelength (λ).

$$\lambda = \frac{343.85\ m/s}{40000\ Hz} = 8.5\ mm \quad (36)$$

The Ultrasonic sensor will also discern barriers that are greater than 8.5 mm in wave length. Once an ultrasonic sensor detects impacts with any barrier in the AUV direction, the echo of this barrier will reflect back to the ultrasonic sensor receiver. Which indicates, across AUV direction there is a barrier. A time discrepancy between both the signals received and the signals transmitted is being used to evaluate the range (d) between both the ASV and the barrier as follows Eq. (37).

$$d = (T * C_s)/2 \quad (37)$$

where: d is the measured distance in cm, T is a time in µsec. The control system of AUV is shown in Fig. 17.

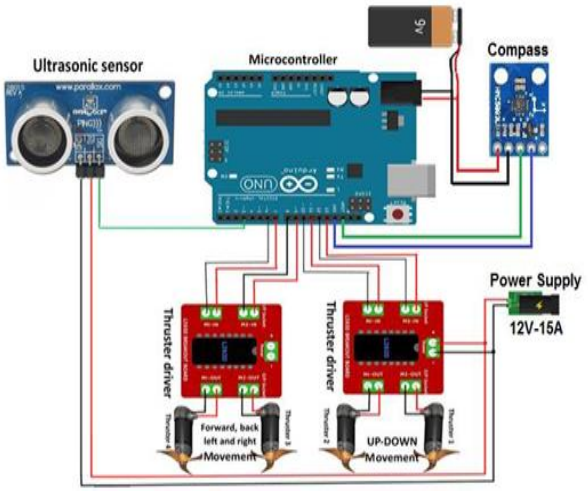


Fig. 17. Control system of AUV.

### B. GUIDANCE Algorithmic of AUV

In dangerous and disastrous environments, the AUV is preprogrammed to dive and sail from Base station ($B_P$) to Target position ($T_P$) to execute the required tasks efficiently and return back without any external control from base station [24]. [25].So there are necessary parameters to be obtains. These parameters include, the current position ($C_P$) of AUV, the target position ($T_P$), the angle ($\Theta_c$) between the $C_P$ of AUV and North pole, the distance (d) and direction angle ($\Theta_d$) between $C_P$ of AUV and $T_P$, and the movement angle ($\Theta_m$) between $C_P$ of AUV and $T_P$. The AUV is designed according to the following:-

- Send AUV from the base station to goal position to perform multiple tasks like surveillance, rescue and tracking. Instantaneously, the direction taken by AUV is stored in AUV memory.
- After implementing the tasks, AUV returns back to base station according to the stored path in its memory.

#### 1) AUV Sending of Base Station (BP) to Target (TP)

A simple model for sending the AUV from $B_P$ to $T_P$, in addition to the necessary parameters, is represented in Fig. 18.

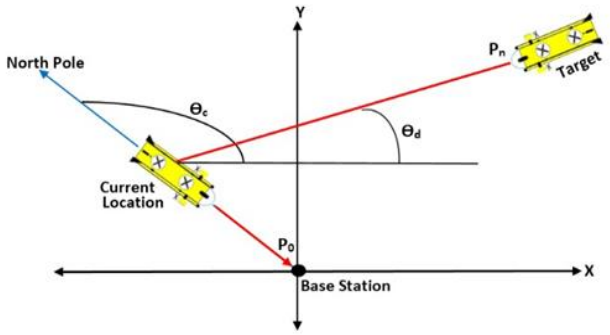


Fig. 18. Flowchart of sending and storing path.

The sending steps are followed:

- Diving AUV to required depth of target position.
- Using compass sensor to determine the angle ($\Theta_c$) between the present AUV ($C_P$) location of AUV and North Pole location.
- The angle of direction ($\theta_d$) between the current location of AUV ($C_{P_{lat}}$,$C_{P_{lon}}$) and target position ($T_{P_{lat}}$,$T_{P_{lon}}$) is given by Eq. (38).

$$.\Theta_d = a\,tan\,2\,(X,Y) \tag{38}$$

where

$$X = \cos(T_{P_{lat}}) * \sin(T_{P_{lon}} - C_{P_{lon}})$$
$$Y = \cos(C_{P_{lat}}) * \sin(T_{P_{lat}}) - \sin(C_{P_{lat}}) * \cos(T_{P_{lat}}) * \cos(T_{P_{lon}} - C_{P_{lon}})$$

- The movement angle ($\Theta m$) between CP of AUV and TP is determined by Eq. (39).

$$.\Theta_m = \Theta_c - \Theta_d \tag{39}$$

where: $\theta_c$ is the north angle between both present AUV location and the North Pole location, $\theta_d$ is the angle of direction between the actual AUV location and the goal location, and movement angle ($\Theta_m$) is used to rotate ASV to the right direction.

- The distance (d) between target position (TP) and current position (CP) of AUV is determined by Haverise formula [26] as the following Eq. (40).

$$d = 2R_e * arc\sin\left(\sqrt{sin^2\left(T_{P_{lat}} - C_{P_{lat}}/2\right)} + \sqrt{\cos\left(T_{P_{lat}}\right) * \cos\left(C_{P_{lat}}\right) * sin^2\left(T_{P_{lon}} - C_{P_{lon}}/2\right)}\right) \tag{40}$$

where: d is the distance between the target location and the current location of AUV, and $R_e$ is earth's radius= 6.317km.

The sending and storing path flowchart of AUV is shown in Fig. 19.

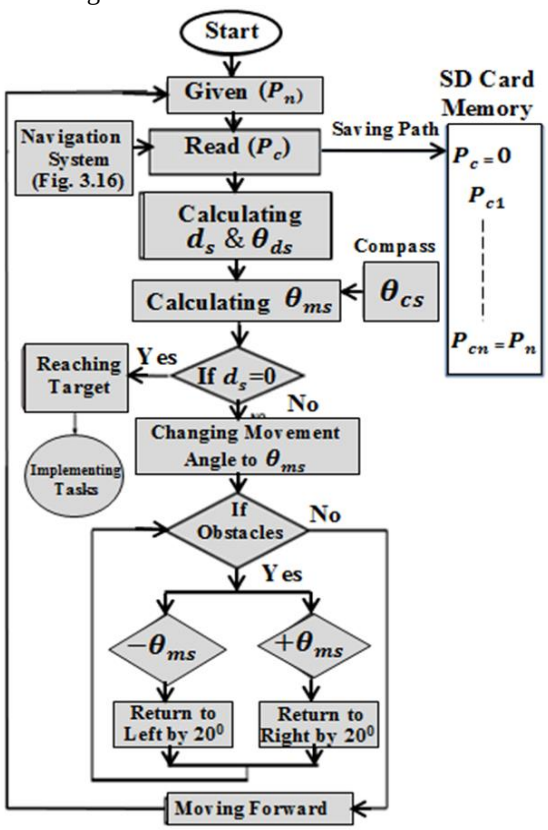


Fig. 19. Flowchart of sending AUV and path storing.

#### 2) Return AUV Back from Target (TP) to Base Station (BP)

A simplified diagram of return AUV back from $T_P$ to $B_P$, in addition to the necessary parameters, is represented in Fig. 20.

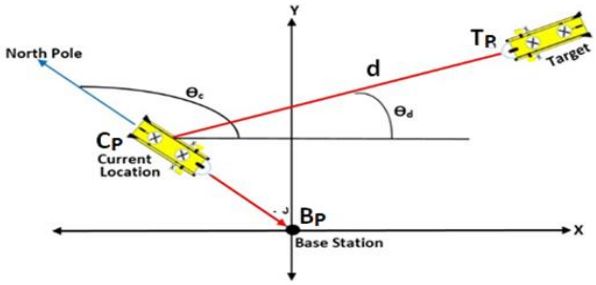


Fig. 20. Flowchart of return AUV back path.

It the return AUV steps are followed:-

- A compass sensor is using to measure the angle ($\boldsymbol{\Theta}_c$) between Target position ($\mathbf{T}_P = \boldsymbol{C}_{P_n}$) and North Pole.
- Reading next position ($\boldsymbol{C}_{P_{n-1}}$) from memory of AUV.
- The direction angle ($\boldsymbol{\theta}_d$) between the current position of AUV ($\boldsymbol{C}_{P_{nlat}}$ , $\boldsymbol{C}_{\boldsymbol{P_{nlon}}}$) and the next position ($\boldsymbol{C}_{P_{nlat-1}}$ , $\boldsymbol{C}_{\boldsymbol{P_{nlon-1}}}$) from the AUV memory gives by Eq. (41).

$$.\Theta_d = a\,tan\,2\,(X,Y) \tag{41}$$

where

$$X = \cos(C_{P_{nlat-1}}) * \sin(C_{P_{nlon-1}} - C_{P_{nlon}})$$

$$Y = \cos(C_{P_{nlat-1}}) * \sin(C_{P_{nlat-1}}) - \sin(C_{P_{nlat}}) * \cos(C_{P_{nlat-1}}) * \cos(C_{P_{nlon-1}} - C_{P_{nlon}})$$

- The movement angle ($\Theta_m$) can be calculated by following Eq. (42).

$$.\Theta_m = \Theta_d - \Theta_c \tag{42}$$

where: $\theta_c$ is the angle between the target position of AUV and the North Pole, $\theta_d$ is the direction angle between the target position of AUV and the next position in memory of AUV.

- Haverise equation calculates the (d) among target location ( $\boldsymbol{C}_{P_{nlat}}$ , $\boldsymbol{C}_{\boldsymbol{P_{nlon}}}$ ) and next location ($\boldsymbol{C}_{P_{nlat-1}}$ ,$\boldsymbol{C}_{\boldsymbol{P_{nlon-1}}}$) from AUV memory. The Haverise formula is given by Eq. (43).

$$d = 2R_e * arc\sin\left(\sqrt{sin^2\left(C_{P_{nlat-1}} - C_{P_{nlat}}/2\right)} + \sqrt{\cos\left(C_{P_{nlat-1}}\right) * \cos\left(C_{P_{nlat}}\right) * sin^2\left(PC_{P_{nlon-1}} - C_{P_{nlon}}/2\right)}\right) \tag{43}$$

where: d is the distance between the target location and the next location from memory, and $R_e$ is earth's radius=6.317km.

The Returned AUV flowchart is shown in Fig. 21.

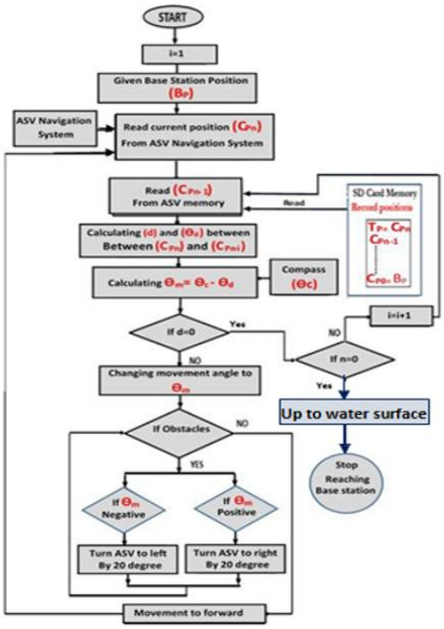


Fig. 21. Flowchart of returning AUV.

## IV. Experimental Works

The designed AUV used in the following tests is shown in Fig. 22 (a). Its details of the overall system are shown in Fig. 22 (b).

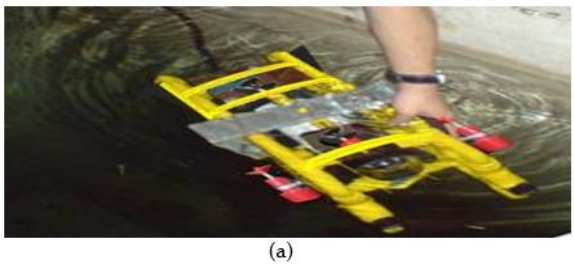

(a)

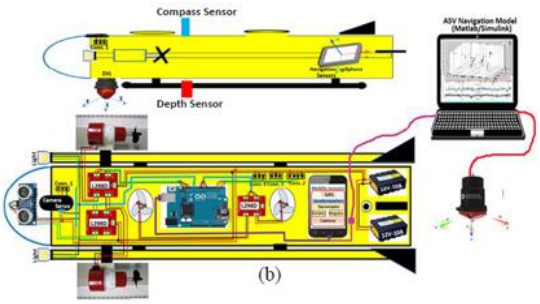


(b)

Fig. 22. Designed AUV and system details.

The efficiency of AUV has been tested at depth of 7 meters from water surface in testbed. The testbed is shown in Fig. 23.

Fig. 23. Testbed.

### A. Test 1: Sending AUV to Target Located at Depth of 7 Meters from Water Surface

In this test, the target ($T_P$) is located at depth of 7 meters from water surface. After that, the AUV sent automatically from the Base station ($B_P$) on water surface to the target position ($T_P$) to test its efficiency. In the same time, the path taken by the AUV is stored in AUV memory. This path is plotted with the Matlab program as shown in Fig. 24.

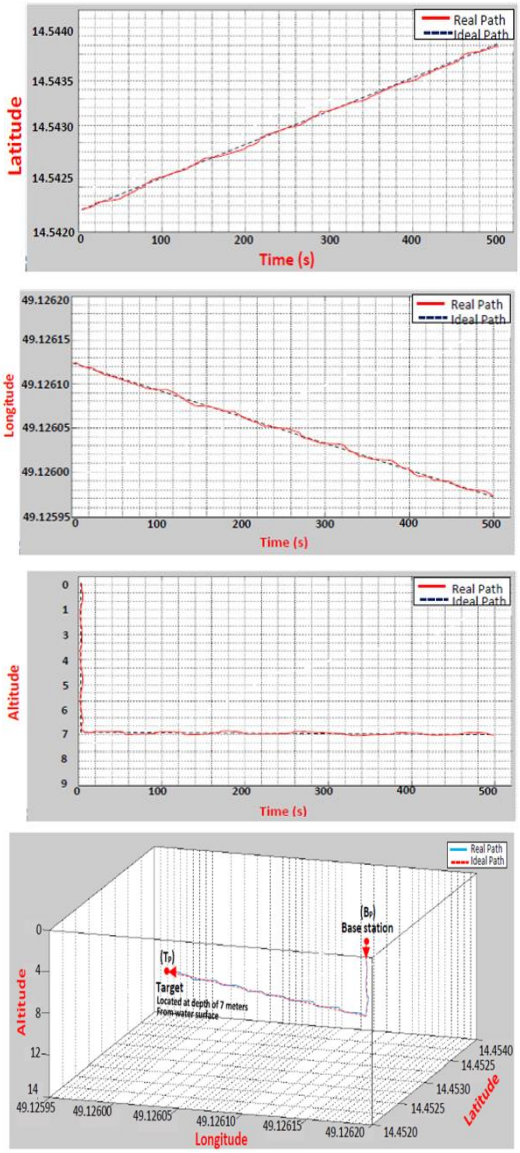


Fig. 24. The path taken by AUV to reach the target located surface.

In test1, the estimated errors of latitude, longitude, and altitude relative to ideal path are shown in Fig. 25.

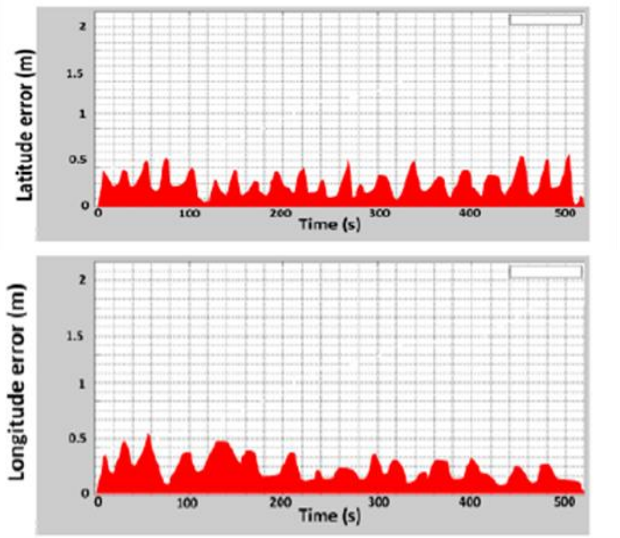


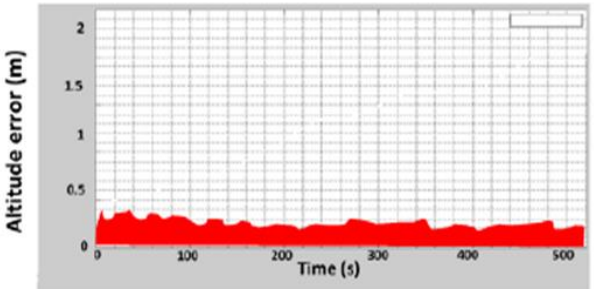


Fig. 25. Estimated errors of latitude, longitude, and altitude relative to ideal path.

From test1, the maximum estimated errors of latitude, longitude, altitude, and position relative to ideal path are shown in Table II.

TABLE II: MAXIMUM ERRORS OF LATITUDE, LONGITUDE, ALTITUDE AND POSITION RELATIVE TO IDEAL PATH

| | Maximum Errors (m) |
|---|---|
| Latitude | 0.4975 |
| longitude | 0.52741 |
| Altitude | 0.3672 |
| Position | 0.61234 |

### *B. Test2: Placing Three Obstacles in Path of AUV*

Throughout this study, the AUV route comprises three barriers. After that The AUV sent automatically from the Base station ($B_P$) on water surface to Target position ($T_P$) to test its efficiency. In the same time, the path taken by the AUV is stored in AUV memory. This path is plotted with the Matlab program as shown in Fig. 26

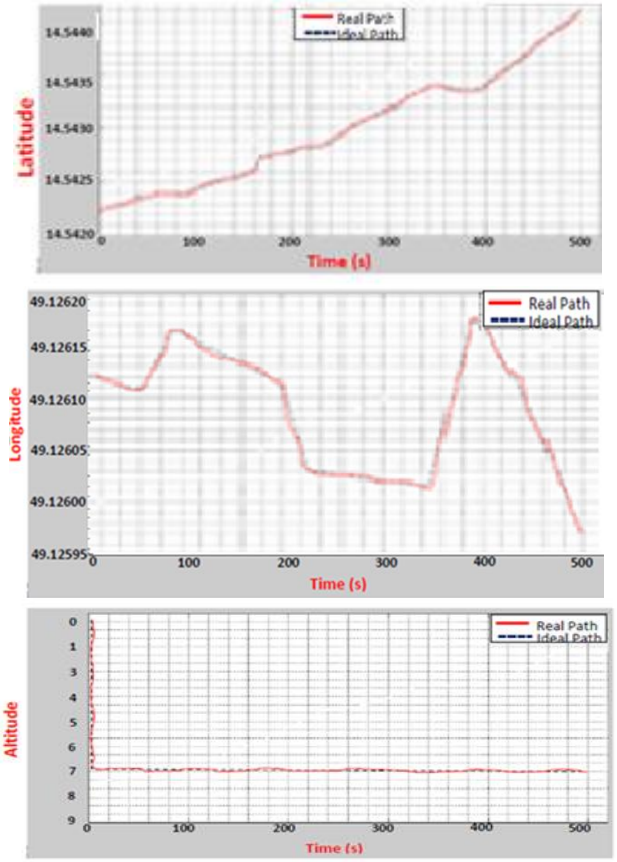

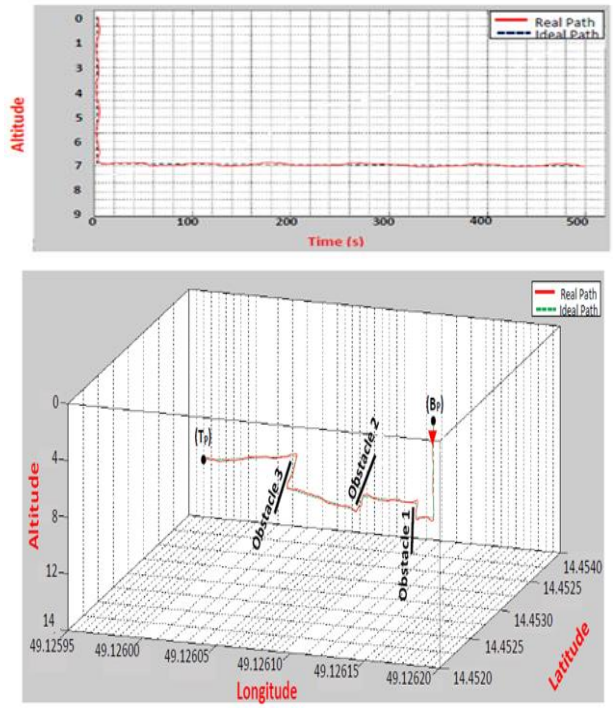


Fig. 26. The path taken by AUV to reach the target with three obstacles.

In test2, the estimated errors of latitude, longitude, and altitude relative to ideal path are shown in Fig. 27.

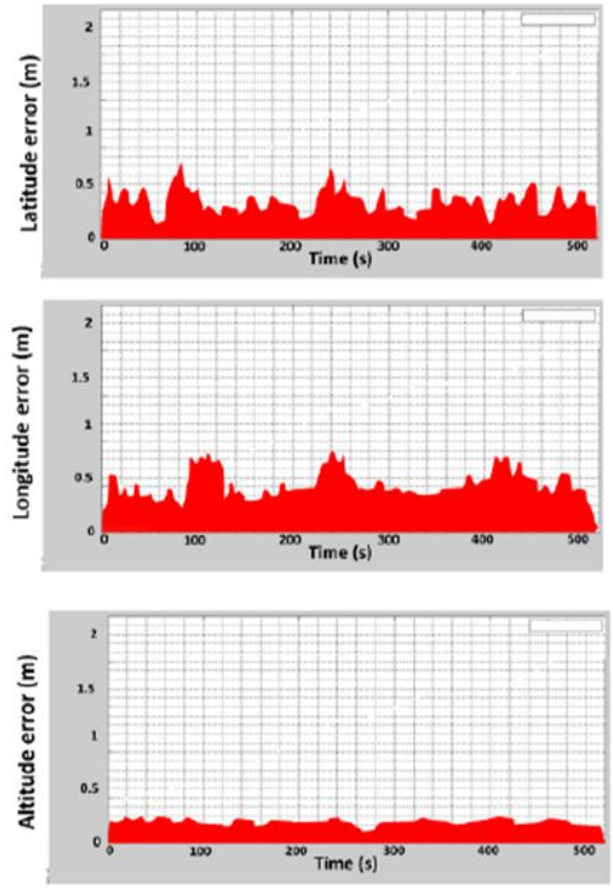


Fig. 27. Estimated errors of latitude, longitude, and altitude relative to ideal path.

From Fig. 27, the maximum estimated errors of latitude, longitude, and location through GPS blackouts are shown in Table III.

TABLE III: MAXIMUM ERRORS OF LATITUDE, LONGITUDE, ALTITUDE AND POSITION RELATIVE TO IDEAL PATH

| | Maximum Errors (m) |
|---|---|
| Latitude | 0.6321 |
| longitude | 0.78341 |
| Altitude | 0.3214 |
| Position | 0.81235 |

### C. *Test3: Returning AUV Back to Base Station According to the Memory Stored Route*

In this test, **changed obstacle 1 location and obstacle 2 location.** After that the AUV return back from target location to base station according to the route saved into its memory. The return path taken by AUV is plotted with the Matlab program as shown as shown in Fig. 28.

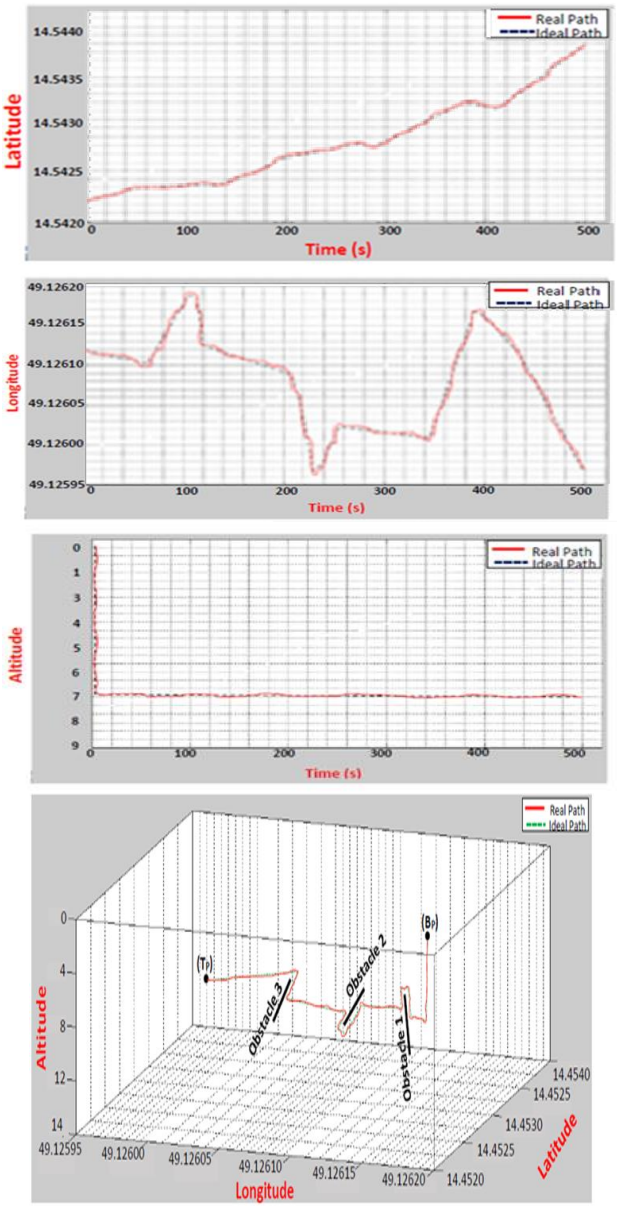


Fig. 28. Return path taken by AUV according to Stored Path in its Memory.

From test3, the calculated errors of latitude, longitude, and altitude relative to ideal path are shown in Fig. 29.

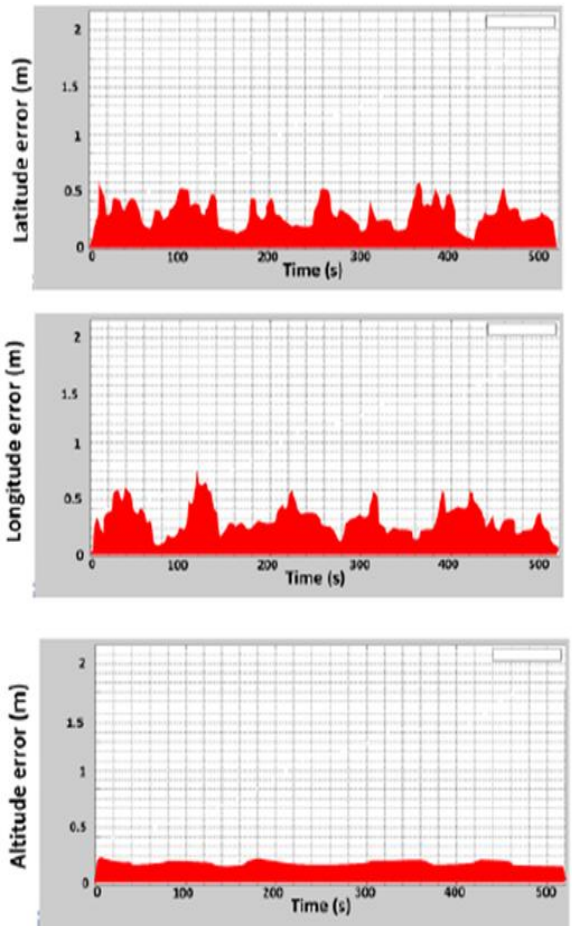


Fig. 29. Estimated errors of latitude, longitude, and altitude relative to ideal path.

From Fig. 29, the maximum estimated errors of latitude, longitude, and are shown in Table IV.

TABLE IV: MAXIMUM ERRORS OF LATITUDE, LONGITUDE, ALTITUDE AND POSITION RELATIVE TO IDEAL PATH

| | Maximum Errors (m) |
|---|---|
| Latitude | 0.5143 |
| longitude | 0.698321 |
| Altitude | 0.376432 |
| Position | 0.71563 |

During test3, although there are changing in the locations of obstacle 1 and obstacle2, the AUV could be returning to base station with highly efficient.

## V. CONCLUSION

Our proposed method to improve a navigation and guidance system of AUV is able to provide a reliable navigation and guidance solution of AUV. The AUV is able to reach the target location with high efficiency. After that, the ASV is able to re-turn to the base station according to the stored route from its memory with highly efficient also. In addition, our proposed navigation and guidance method can reduce cost and provide a suitable size for most AUVs. Finally, it is a useful platform to develop new future skills and implement more difficult tasks.

## CONFLICT OF INTEREST

"The authors declare no conflict of interest".

## AUTHOR CONTRIBUTIONS

Authors Hatem A. Khater, Ashraf .Elsayed and Noha. El-Shoafy conducted the research; Hatem A. Khater, Ashraf .Elsayed and Noha. El-Shoafy analyzed the data; Noha. El-Shoafy wrote the paper; all authors had approved the final version.

## ACKNOWLEDGMENT

My sincere gratefulness for constructive supervision; Dr. Hatem for his continuous advices,

I am extremely grateful to my creative supervisor; Dr. Ashraf El-Sayed, who provided support, and constructive comments throughout the entire project.

Finally yet importantly, I want to thank my family for their prayers and their continuous support.

## REFERENCES

[1] O. Czogall and S. Naumann, "Pedestrian guidance for public transport users in indoor stations using smartphones," in *Proc. IEEE 18th International Conference on Intelligent Transportation Systems*, Las Palmas, Spain, Sept. 2015, pp. 2539-2544.

[2] A. Tal, I. Klein, and R. Katz, "Inertial Navigation System/Doppler Velocity Log (INS/DVL) fusion with partial DVL measurements," *Sensors Journal, MDPI*, vol. 8, no 5, pp. 12-32, February 2017.

[3] K. S. Alli, M. O. Onibonoje, A. S. Oluwole, M. A. Ogunlade, A. C. Mmonyi, O. Ayamolowo, and S. O. Dada, "Development of an arduino-based obstacle avoidance robotic system for an unmanned vehicle," *ARPN Journal of Engineering and Applied Sciences*, vol. 13, N0. 3, pp. 886-892, Feb. 2018.

[4] F. Tabassum, S. Lopa, M. M. Tarek, and B. J. Ferdosi, "Obstacle avoiding robot," *Global Journal of Researches in Engineering: H Robotics & Nano-Tech*, vol. 17, no. 1, pp. 18-24, 2017.

[5] Y. Zhao, "GPS/IMU integrated system for land vehicle navigation based on MEMS," *Licentiate thesis in Geodesy, Royal Institute of Technology (KTH) Division of Geodesy and Geoinformatics*, Stockholm, Sweden, September 2011.

[6] A. Noureldin, T. B. Karamat, and J. Georgy, *Fundamentals of Inertial Navigation, Satellite based Positioning and Their Integration*, Springer Publication, Hardcover, 2013.

[7] W. Yan, L. Wang, Y. Jin, and G. Shi, "High accuracy navigation system using GPS and INS system," in *Proc. 6th Annual IEEE International Conference on Cyber Technology in Automation, Control and Intelligent Systems*, Chengdu, China, June 2016, pp. 365 – 369.

[8] Y. Yoon, K. H. H. Li, J. S. Lee, and W. T. Park, "Real-time precision pedestrian navigation solution using inertial

navigation system and global positioning system," *Advances in Mechanical Engineering*, vol. 2, no. 5, pp. 1–9, April 2016.
[9] K. Pan, M. Ren, P. Wang, and Y. Liu, "A federated filtering personal navigation algorithm based on MEMS-INS/GPS integrated," in *Proc. 28th Chinese Control and Decision Conference (CCDC)*, Yinchuan, China, May 2016, pp. 5237 – 5241.
[10] Q. Hegrenæs, A. Ramstady, T. Pederseny, and D. Velasco, "Validation of a new generation DVL for underwater vehicle navigation," *Kongsberg Maritime Subsea, Marine Robotics Department*, Horten, Norway, 2016.
[11] L. Chunjing, W. Bo, D. Zhihong, and F. Mengyin, "In-motion initial alignment method for DVL-aided SINS under wave disturbance for AUV," in *Proc. 33rd Chinese Control Conference*, Nanjing, China, 28-30 July 2014, pp. 658-663.
[12] A. Rossi, M. Pasquali, and M. Pastore, "Performance analysis of an inertial navigation algorithm with DVL auto-calibration for underwater vehicle," *Inertial Sensors and Systems*, Karlsruhe, Germany, Sept. 2014, pp. 1–19.
[13] Hoskinson and E. J. Park, "Integration of MEMS inertial and pressure sensors for vertical trajectory determination," *IEEE Transactions on Instrumentation and Measurement*, vol. 64, no. 3, pp. 804–814, March 2015.
[14] H. Khater, M. Zakria, and A. Bahasan, "GPS/DVL/ MEMS-INS smartphone sensors integrated method to enhance autonomous navigation, guidance and control system of AUSVs based on ADSF combined filter data fusion," *Journal of the International Measurement Confederation*, July 2019.
[15] H. Khater, M. Zakria, and A. Bahasan, "GPS/DVL/ MEMS-INS smartphone sensors integrated method to enhance USV navigation system based on adaptive DSFCF," *IET Radar, Sonar & Navigation*, June 2019.
[16] N. K. Yong, S. Jeong, and H. T. Choi, "Navigation of an underwater vehicle using ahrs and depth sensor," in *Proc. 15th International Conference on Control, Automation and Systems (ICCAS)*, Busan, South Korea, Oct. 2015, pp. 482-484.
[17] A Publication of the National Wildfire Coordinating Group, "Basic Land Navigation," National Incident Management System, NWCG Operations and Training Committee, May 2016.
[18] H. Tao, "Object tracking and kalman filtering," Department of Computer Engineering, the University of California at Santa Cruz, California, USA, 2015.
[19] Z. Chen, Y. Qu, X. Ling, Y. Li, H. Jiao, and Y. Liu, "Study on GPS/INS loose and tight coupling," in *Proc. International Conference on Intelligent Human-Machine Systems and Cybernetics*, Hangzhou, China, Aug. 2015, pp. 34-37.
[20] S. Luitel, "Design and Implementation of a Smart Home System," Master thesis, Information Technology, Helsinki Metropolia University of Applied Sciences, August 2013.
[21] K. M. Raza, M. Kamil, and P. Kumar, "Speed control of DC Motor by using PWM," *International Journal of Advanced Research in Computer and Communication Engineering*, vol. 5, no. 4, pp. 307-309, April 2016.
[22] C. H. N. Soni, C. H. Sarita, S. Maheshwari, B. K. Sahu, B. Jain, and G. Shrivastava, "Obstacle avoiding robot," *International Journal of Engineering Science and Computing*, vol. 7, no. 3, pp. 5991-5992, March 2017.
[23] H. Khater, M. Zakria, and A. Bahasan, "A novel GPS/RAVO/MEMS-INS smartphone sensors integrated method to enhance USV navigation system during GPS outages," *Journal of Measurement Science and Technology*, June 2019.
[24] H. Khater, S. Mesbah, and A. Anwar, "Enhanced navigation system for AUV using mobile application," *Int. J. Eng. Inventions*, vol. 5, no. 1, pp. 14–19, 2015.
[25] A. H. Khater and A. Michle, "Using novel technologies in unmanned underwater vehicle," *Int. J. Electr. Electron*, vol. 11, no. 9, pp. 184–187, 2014.



**Dr. Hatem A. Khater** received BSc. In Electrical Engineering, MSc. IN Electronic and Communication Engineering and Ph.D. in Computer Engineering, Kent University, United Kingdom, in 2008. He is Associate Professor, Head of Mechatronics dept., Faculty of Engineering, Horus University and lecturere (Part Time) at the Arab Academy for Science and Technology (AASTMT), Computer Engineering Department, Electronic Communication Engineering Department, College of Engineering and Technology, College of Computing & Information Technology, Walls University. In addition, he holds the position of Director of Naval Technical & Research and Development Department. His research interests include AI, Computer Vision, DSP, Software Engineering, cryptograph, Image Feature Detection, Matching Technique,, Geometric Transformation, Image Registration, Pattern Recognition, Computer Graphics, Web Programming, Automatic Controls, Modern Electronics communication, Acoustics, Voice Identifications, GIS, International and European Business, Economics & Management information Systems. Member and Reviewer at IET. Also Member of Image and Information Engineering Research Group, University of Kent, U.K.

**Dr. Ashraf A. Elsayed** received B.S. degree from the Alexandria University, Alexandria, Egypt, in 1995, the M.S. degree from the Alexandria University, Alexandria, Egypt, in 2004, both in Computer science. And the Ph.D degree from the University of Liverpool, UK, in 2012, in Computer science.His currently position: Assistant Professor at Zewail city of Science and Technology. (On leave from Assistant Professor at Faculty of Science - Alexandria university, Alexandria, Egypt) .His research interests include Data Science - Big data Analytics - Deep learning.

**Noha N. El - Shoafy** received B.S. degree from the Alexandria University, Alexandria, Egypt, in 2005, the M.S. degree from from Arab Academy for Science and Technology, Alexandria, Egypt, in 2012, both in Computer science. She is currently pursuing the Ph.D. degree with the Department of Computer Science and Mathematics, from Faculty of Science, Alexandria University, Egypt.She holds the position of Coordinator of both Computer Science and Information tecknology department at King Khalid University, Saudi Arabia.
Her research interests include Software Engineering, Mobile Application, Automatic Controls, GIS.